

Phase equilibrium of the Cu–Fe–O system under Ar, CO₂ and Ar+0.5% O₂ atmospheres during CuFeO₂ single-crystal growth

T.-R. ZHAO, M. HASEGAWA, H. TAKEI

Institute for Solid State Physics, University of Tokyo, 7-22-1, Roppongi, Minato-ku, Tokyo 106, Japan

Phase relations of CuFeO₂ during crystal growth under Ar, CO₂ and Ar + 0.5% O₂ surrounding atmospheres have been investigated using scanning electron microscopy together with electron probe microanalysis and X-ray powder diffraction. CuFeO₂ was found to partially decompose into Fe₂O₃ and Cu₂O before melting and the crystal growth process was by means of Cu₂O-solvent movement. Under Ar and CO₂ atmospheres, Cu₂O was found to be further reduced to metallic copper, and under CO₂ more severe reduction of copper was observed. No copper reduction could be found under an Ar + 0.5% O₂ surrounding atmosphere.

1. Introduction

CuFeO₂ is a typical compound in the Cu–Fe–O ternary system which was historically the first compound known to exhibit the so-called delafossite structure [1, 2]. The preparation of CuFeO₂ single crystal on a large scale is of interest, because of its structural anisotropy, which causes its anisotropic physical and chemical properties [2–6]. As CuFeO₂ melts incongruently [7], and liquid copper(I) oxides attack all known crucible materials [8], it is very difficult to grow bulk CuFeO₂ single crystals. We have first successfully grown large CuFeO₂ single crystals by using the floating-zone technique [7, 9].

However, as CuFeO₂ is composed of two transition metal oxides of copper and iron, the valence states of the metallic ions depend on various factors such as the ratio of the metallic ion concentrations, the growth temperature and the surrounding atmosphere [10]. Although some studies concerning the oxidation kinetics of CuFeO₂ and phase equilibria of the Cu–Fe–O system have been reported [11–15], no studies on the reduction of this compound at high temperature have been published.

The purpose of the present work was to study the influence of the surrounding atmosphere on the phase equilibrium of CuFeO₂ during crystal growth.

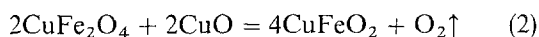
2 Experimental procedure

2.1. Sample preparation

As starting materials, powders of CuO (99.9%, Kojundo Chemicals) and Fe₂O₃ (regent grade, Kanto Chemical Co., Inc.) were well mixed in the ratio 2:1 and pre-fired at 800 °C for 15 h in a flow of air (20 ml min⁻¹) at a heating rate of 1.5 °C min⁻¹



The pre-fired products were mixed again and filled into an alumina boat, which was introduced into an alumina vacuum reaction furnace (Type SPSH-37, Shiriko-nitto Konetsu Kogyo Co., Ltd) and heated to 950 °C at a heating rate of 1.5 °C min⁻¹. The solid-state reaction between CuFe₂O₄ and CuO was carried out at 950 °C for 24 h in a flow of nitrogen gas (< 20 ml min⁻¹)



CuFeO₂ single phase was confirmed by XRD and no extraneous phase was found.

The cylindrical ceramic rods, 8–10 mm diameter and 60–70 mm long, were formed from the synthesized CuFeO₂ powder by hydrostatic compression and were sintered again in argon gas at 1000 °C for 15 h to increase the density of the rod.

2.2. Crystal growth

The crystal growth was carried out in an infrared radiation furnace, which was described elsewhere [7, 9]. The feed and seed rods were rotated at 15 r.p.m., respectively, and both rods were moved downwards giving a growth speed of 2 mm h⁻¹. To prevent the oxidation of copper ions from Cu⁺ to Cu²⁺, or the reduction of Cu⁺ to Cu or Fe³⁺ to Fe²⁺, crystal growth was carried out in neutral, slightly reducing or oxidizing atmospheres: Ar, CO₂ and Ar + 0.5% O₂ gas in a flow of less than 200 ml min⁻¹, respectively.

As-grown crystals were black and opaque in appearance with the size 8 mm diameter and 20–30 mm long. The CuFeO₂ structure of the crystals was confirmed by means of X-ray powder diffraction (XRD).

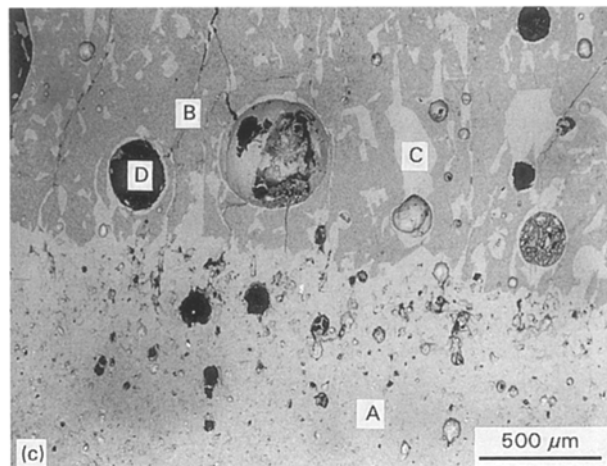
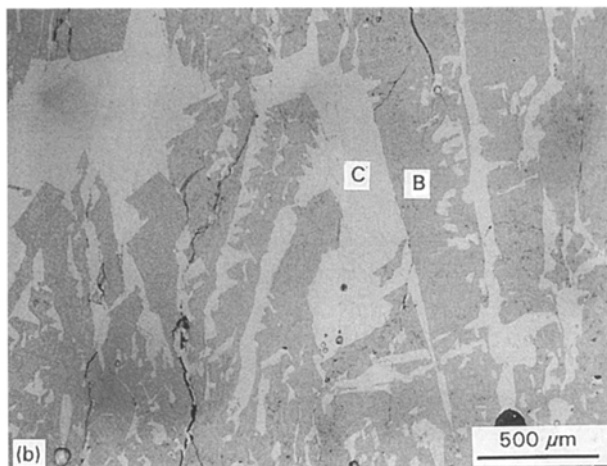
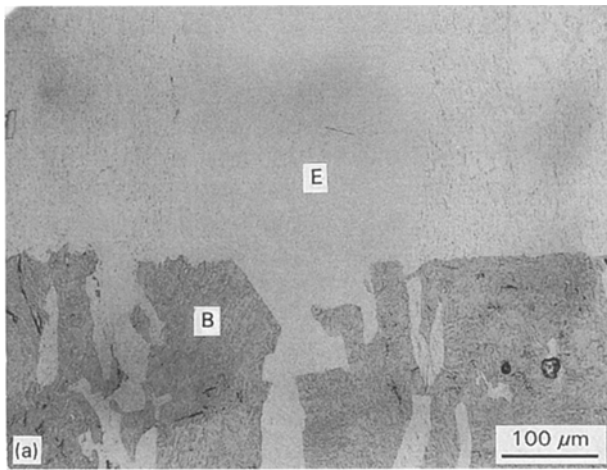
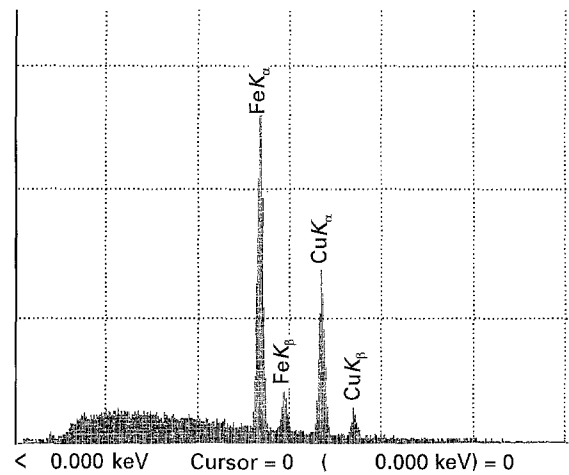


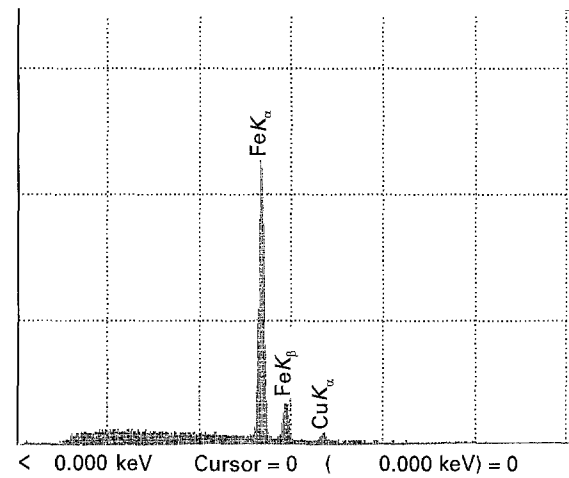
Figure 1 BEI-COMPO photographs of the low-temperature part of the seed rod and crystal interface under an argon atmosphere. (a) The interface of the Fe_2O_3 -rich part and the CuFeO_2 crystal, (b) the Fe_2O_3 -rich region, and (c) the interface of CuFeO_2 seed rod ceramics and the Fe_2O_3 -rich part. A, CuFeO_2 rod ceramics; B, Fe_2O_3 ; C, CuFeO_2 polycrystals; D, hole; E, CuFeO_2 single crystal.

2.3. Phase analyses

Specimens for phase analyses were prepared from the quenched crystals after the growth temperature was decreased to room temperature at the rate of $15^\circ\text{C min}^{-1}$. The parts containing the interface of the growing crystal and the melting zone, the interface of the growing crystal and the seed rod, or the interface



(a)



(b)

Figure 2 EPMA spectra of (a) CuFeO_2 single crystal and (b) the Fe_2O_3 -rich region.

of the melting zone and the feed rod, were cut along the elongation axis, embedded in resin, lapped with sandpaper and polished with diamond slurry of decreasing coarseness. The back-scattered electron image of the component (BEI-COMPO) was used to observe the morphology. The compositional analysis was carried using electron probe microanalysis (EPMA), and XRD was used to identify the structure of different parts of the samples.

3. Results and discussion

3.1. Phase equilibria of CuFeO_2 under an argon atmosphere

Fig. 1 shows SEM (COMPO) results of the low-temperature part of the seed rod, the interface of the rod and the crystal. Compositional and structural analyses corresponding to these three parts are shown in Figs 2 and 3. Fig. 1a shows the interface of CuFeO_2 crystal (E) and an Fe_2O_3 -rich area (B). It should be noted that Fe_2O_3 suddenly disappeared at the interface. Fig. 1b shows a part composed of Fe_2O_3 (B) and CuFeO_2 polycrystals. The interface of the CuFeO_2 seed rod (A) and the Fe_2O_3 -rich area (B) together with CuFeO_2 polycrystals (C) and the holes (D), which were caused by the incomplete densification of the rod ceramics and aggregation at the interface, are shown

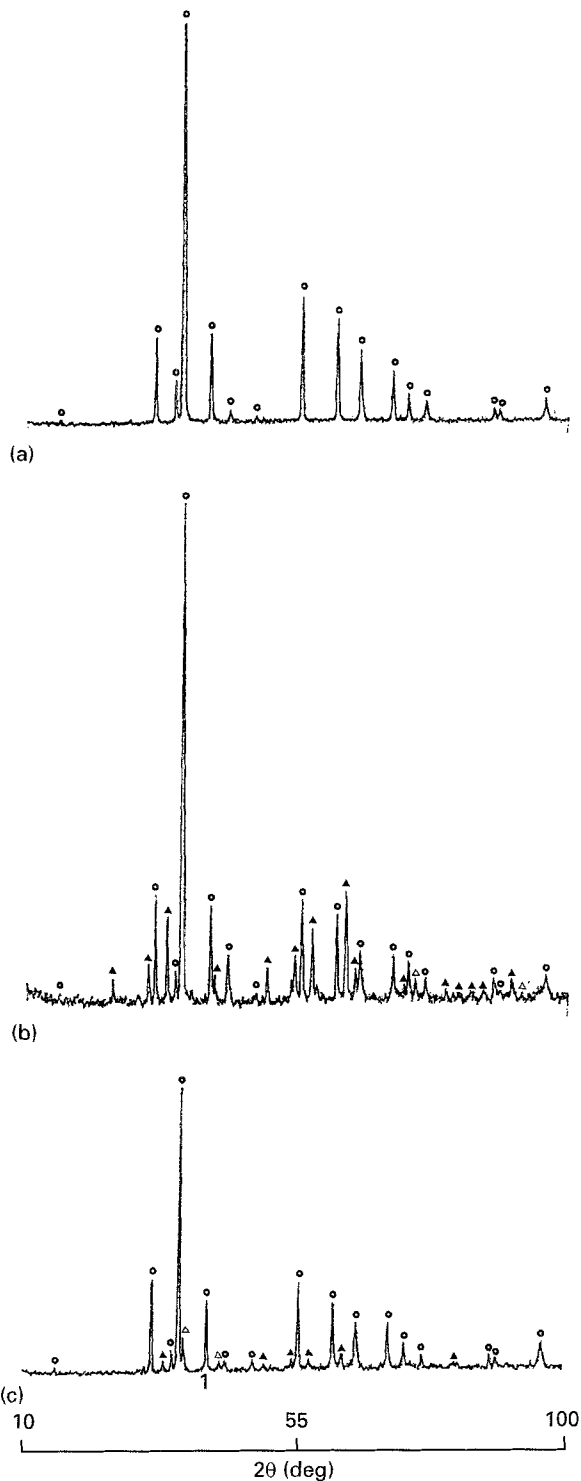


Figure 3 XRD spectra of the low-temperature parts. (a) CuFeO_2 single crystal, (b) Fe_2O_3 -rich region, and (c) the interface of CuFeO_2 seed rod ceramics and the Fe_2O_3 -rich part. (○) CuFeO_2 , (▲) Fe_2O_3 (Δ) Cu_2O .

in Fig. 1c. EPMA and XRD analyses indicated that CuFeO_2 was first decomposed into Fe_2O_3 and Cu_2O before melting, as shown in Figs 2b and 3c. Cu_2O composition was not detected in the Fe_2O_3 -rich region (Fig. 3b), for reasons described later. Figs 2a and 3a show the X-ray spectra of CuFeO_2 single crystal.

The SEM-EPMA and X-ray experiments on the interface of CuFeO_2 single crystal and the melting zone are shown in Figs 4–6. The interfaces of the single crystal (Fig. 4a) and the melting zone (Fig. 4b) were found to be very clearly divided into two parts. EPMA

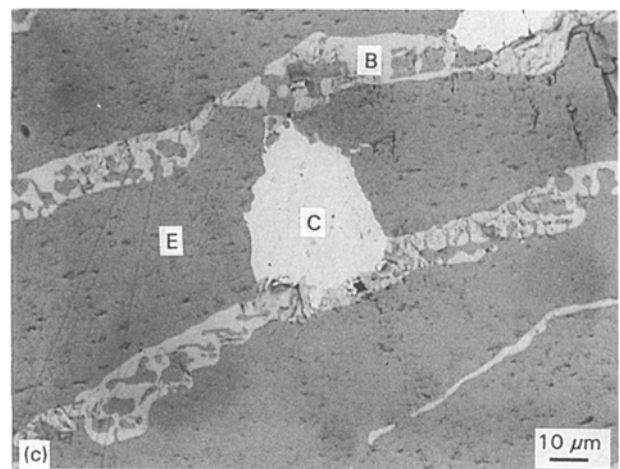
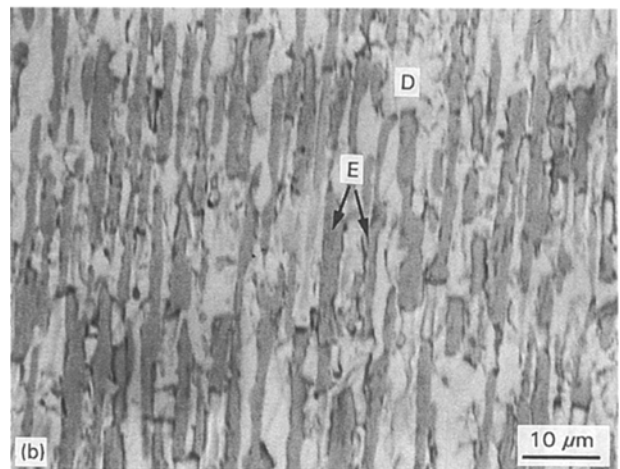
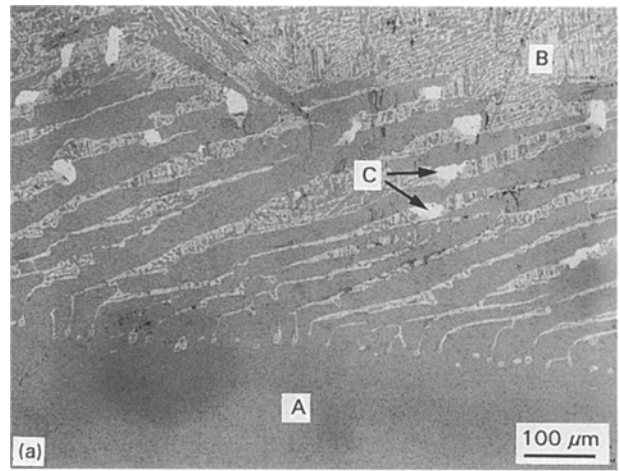


Figure 4 BEI-COMPO photographs of the interface of CuFeO_2 single crystal and the melt under an argon atmosphere. (a) The interface of the CuFeO_2 single crystal and the melting zone, (b) the melt, and (c) reduction of metallic copper. A, CuFeO_2 single crystal; B, Cu_2O -rich region; C, metallic copper; D, Cu_2O ; E, CuFeO_2 polycrystals.

(Fig. 5a) and XRD (Fig. 6a) analyses indicated that there was plenty of Cu_2O at the interface and in the melting zone, which was caused by the decomposition of CuFeO_2 before melting, and Cu_2O tending to move towards the high-temperature region. In addition, there were some inclusions, 20–30 μm in size, at the interface (Fig. 4a and c). EPMA (Fig. 5b) and XRD

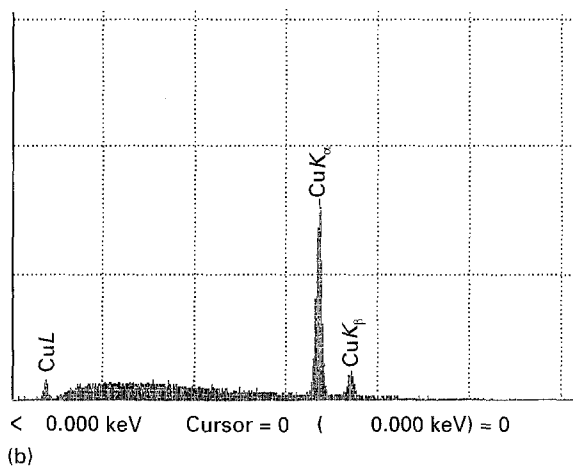
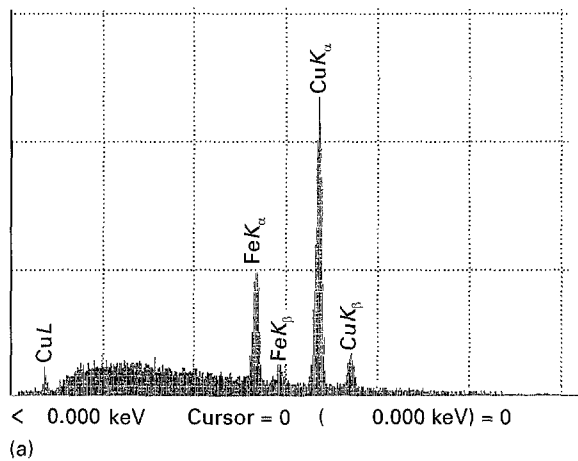


Figure 5 EPMA results of (a) the Cu_2O rich region and (b) metallic copper.

(Fig. 6b) indicated that these particles were of metallic copper, which was considered to arise from further reduction of Cu_2O at high temperature under an argon atmosphere.



The high-temperature part of the feed rod and the interface of the melt and the feed are shown in Fig. 7. The decomposition to Cu_2O also occurred in the melting region (Fig. 7a), and the eutectic crystallization of CuFeO_2 and Cu_2O was observed in the melting region (Fig. 7a and b). In addition, neither Fe_2O_3 nor Cu_2O were found in the feed rod (Fig. 7c).

3.2. Phase equilibria of CuFeO_2 under CO_2 atmosphere

Under a CO_2 surrounding atmosphere, decomposed Cu_2O was found not only in the melting zone but also in the CuFeO_2 feed ceramic region. Fig. 8a shows the feed rod part, in which small white regions, marked B, were observed. X-ray analysis (Fig. 9) indicated that these areas were composed of Cu_2O . Recrystallization of metallic copper with a particle size of about 0.2–0.6 mm diameter also occurred in the melting zone (Fig. 8b). A particle of 30 μm was also observed in the CuFeO_2 seed rod region, as shown in Fig. 8c. EPMA

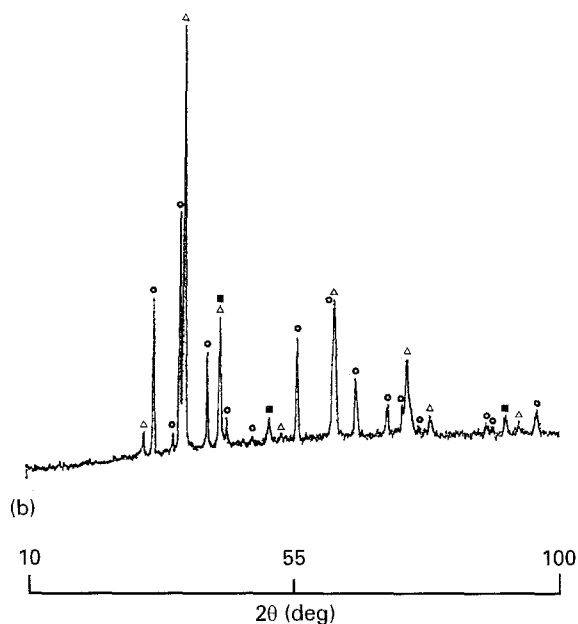
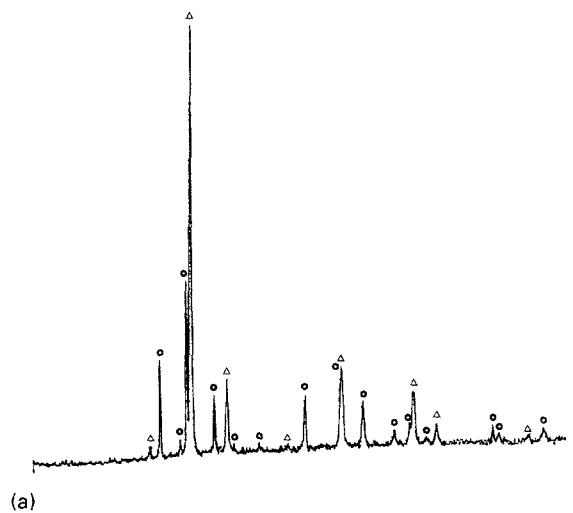


Figure 6 XRD spectra of (a) the Cu_2O -rich part and (b) metallic copper. (○) CuFeO_2 , (△) Cu_2O , (■) Cu.

(Fig. 10) and X-ray analysis (Fig. 9) indicated that its composition was also of copper. It could be considered from the results that the introduction of CO_2 gas caused a reducing condition to be introduced which produces more severe decomposition of Cu_2O and reduction to metallic copper in the sintered rod and melting zone.

3.3. Phase equilibria of CuFeO_2 under an Ar + 0.5% O_2 atmosphere

The CuFeO_2 crystal growth was also carried out under argon gas with 0.5% O_2 . As a result, no metallic copper particles were found either in the melting region or in the feed rod, which indicated that a pure argon surrounding atmosphere is weakly reducing, causing the reduction of metallic copper, whereas the slight addition of oxygen is very effective for suppressing the reduction reaction. No CuO was observed in the melt, sintered rod or crystal.

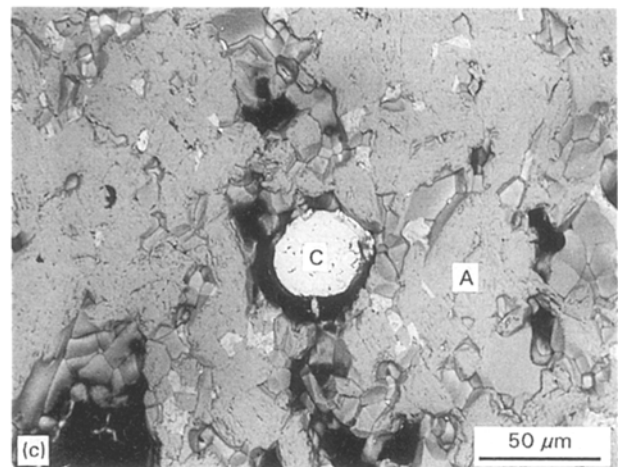
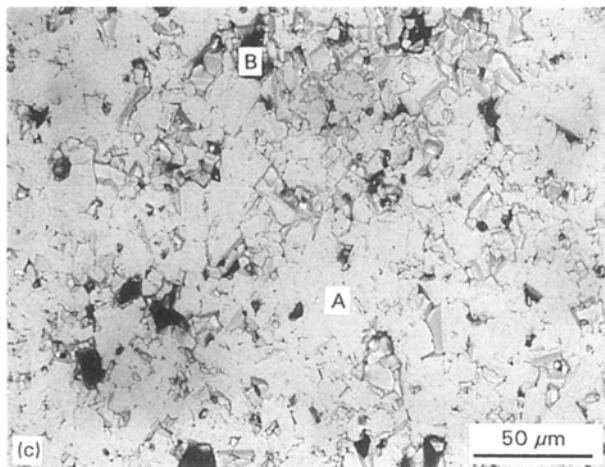
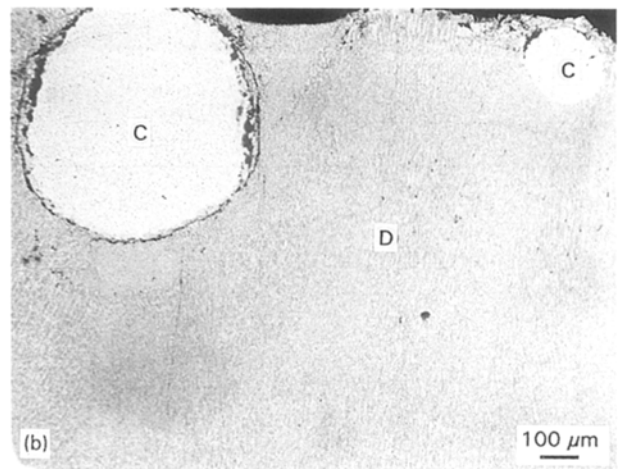
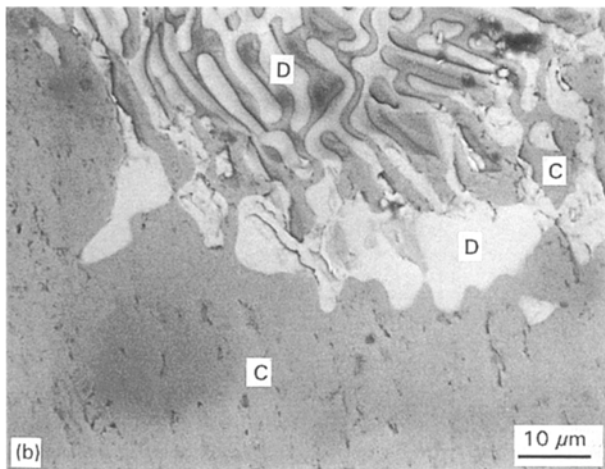
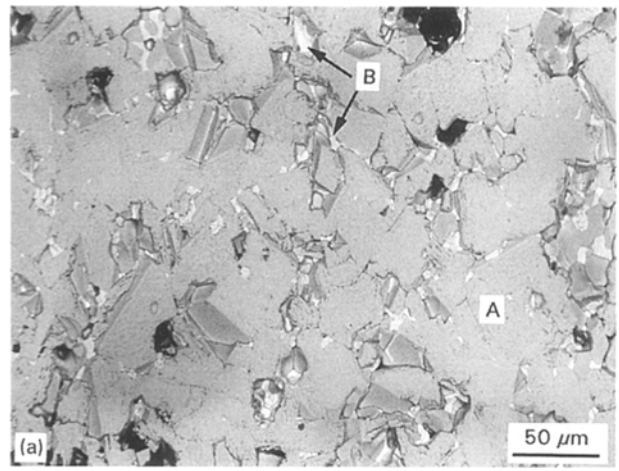
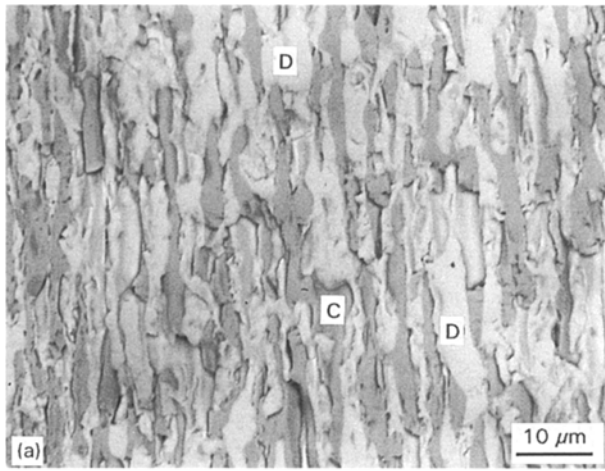


Figure 7 BEI-COMPO photographs of (a) the Cu_2O rich region, (b) the interface of the feed rod and the melt, and (c) the high-temperature part of CuFeO_2 feed rod ceramics. A, CuFeO_2 feed ceramics; B, hole; C, CuFeO_2 polycrystals; D, Cu_2O .

Figure 8 BEI-COMPO results under a CO_2 surrounding atmosphere. (a) CuFeO_2 seed rod ceramics, (b) the melt area, and (c) CuFeO_2 feed rod ceramics. A, CuFeO_2 feed ceramics; B, Cu_2O ; C, metallic copper; D, the Cu_2O -rich region.

3.4. The phase relation of CuFeO_2 at high temperature

From the above results, the phase relation of CuFeO_2 during the floating zone crystal growth at high temperature can be sketched as in Fig. 11. The melted and solidified zone is divided into three parts: a Cu_2O -rich area at the upper side, CuFeO_2 single phase in the middle and a Fe_2O_3 -rich area at the lower side. Fe_2O_3 ,

composition disappeared gradually towards the sintered CuFeO_2 rod because of its high melting point ($T_m = 1550^\circ\text{C}$). On the other hand, Cu_2O melted at relatively low temperature ($T_m = 1230^\circ\text{C}$) and moved upwards as a solvent. This condition allows progress of travelling Cu_2O -solvent growth. The metallic copper appeared under pure argon or CO_2 atmospheres, either in the interface region of the melt and crystal or

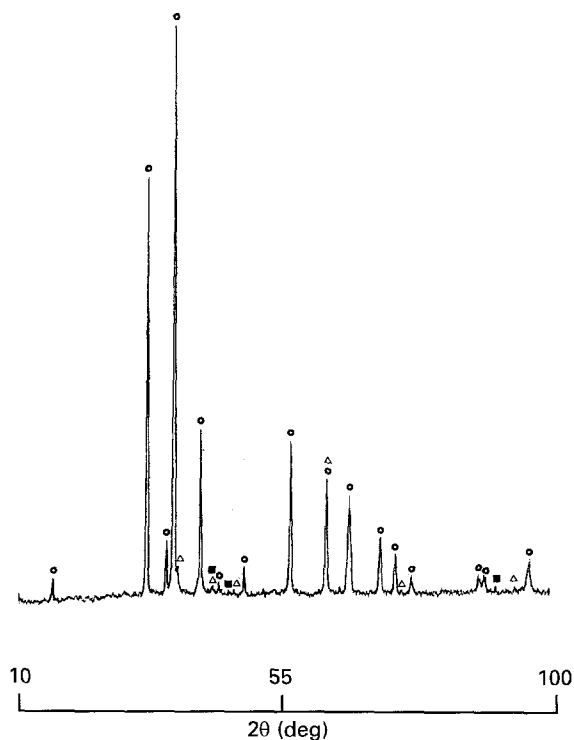


Figure 9 XRD spectrum of CuFeO_2 seed rod under a CO_2 atmosphere. (O) CuFeO_2 , (Δ) Cu_2O , (\blacksquare) Cu.

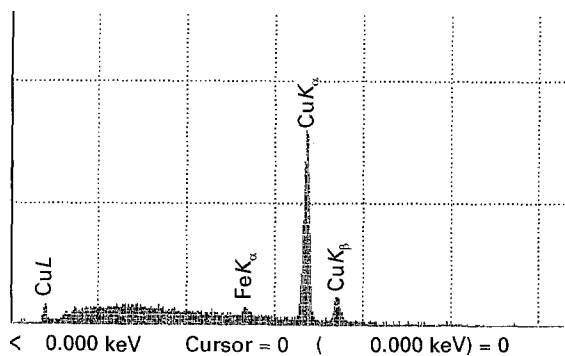


Figure 10 EPMA spectrum of metallic copper in the seed rod.

in the melt by reducing the segregated Cu_2O . A partial phase diagram for the Cu_2O – Fe_2O_3 binary system and a detailed explanation of the phase relation have been given elsewhere [16].

4. Conclusion

The atmospheric conditions of the Cu–Fe–O system were investigated in the travelling Cu_2O –solvent floating-zone growth of CuFeO_2 crystals under Ar, CO_2 and Ar + 0.5% O_2 surrounding atmospheres. The results showed that under argon and CO_2 surrounding atmospheres, the reduction of metallic copper from segregated Cu_2O was found either at the interface of melt and crystal, or in the melting zone, and the latter caused a more severe reduction to metallic copper. Under an Ar + 0.5% O_2 atmosphere, no reduction of metallic copper was found.

These results lead to the conclusion that a slight oxidizing atmosphere is essential for growing good

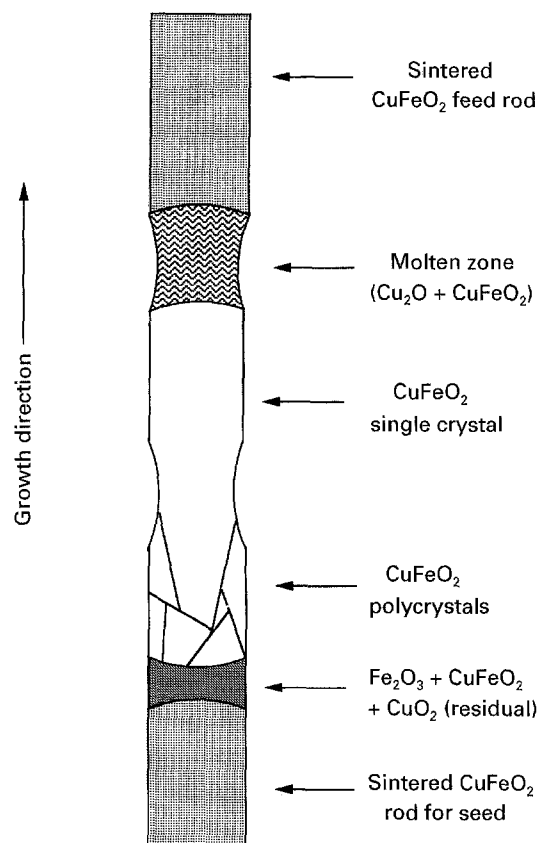


Figure 11 Schematic diagram of the phase relation at high temperature.

single crystals of CuFeO_2 with the stoichiometric valence states of Cu^+ and Fe^{3+} .

Acknowledgements

The authors thank Mr M. Koike for his help in taking care of all equipment and Mrs F. Sakai for her help with the SEM–EPMA experiment. They also thank all colleagues of the laboratory for their helpful discussions and comments.

References

1. E. M. LEVIN, C. R. ROBBINS and H. F. McMURIDE, "Phase Diagrams for Ceramists" (American Ceramic Society, Columbus, OH, 1964) p. 53.
2. P. DORDOR, J. P. CHAMINADE, A. WICHAINCHAI, E. MARQUESTAUT, J. P. DOUMERC, M. POUCHARD and P. HAGENMULLER, *J. Solid State Chem.* **75** (1988) 105.
3. F. A. BENKO and F. P. KOFFYBERG, *J. Phys. Chem. Solids* **48** (1987) 431.
4. C. T. PREWITT, R. D. SHANNON and D. B. ROGERS, *Inorg. Chem.* **10** (1971) 719.
5. S. MITSUDA, H. YOSHIZAWA, N. YAGUCHI and M. MEKATA, *J. Phys. Soc. Jpn* **60** (1991) 1885.
6. M. MEKATA, N. YAGUCHI, T. TAKAGI, T. SUGINO, S. MITSUDA, H. YOSHIZAWA, N. HOSORITO and T. SHINJO, *ibid.* **62** (1993) 4474.
7. T. R. ZHAO, M. HASEGAWA, and H. TAKEI, *J. Crystal Growth*, to be published.
8. R. S. ZUCKER, *J. Electrochem. Soc.* **112** (1965) 417.
9. T. R. ZHAO, M. HASEGAWA, M. KOIKE and H. TAKEI, *J. Crystal Growth* **148** (1995) 189.
10. G. C. JAIN, B. K. DAS and RAM AVTAR, *J. Mater. Sci.* **12** (1977) 1903.

11. *Idem, ibid.* **16** (1981) 102.
12. K. T. JACB, K. FITZNER and C. B. ALCOCK, *Metall. Trans.* **8B** (1977) 451.
13. S. C. SCHAEFER, G. L. HUNDLEY, F. E. BLOCK, R. A. McCUNE and R. V. MRAZEK, *ibid.* **1** (1970) 2557.
14. C. F. JEFFERSON, *J. Appl. Phys.* **36** (1965) 1165.
15. ZDENEK SIMSA, *IEEE Trans. Magn.* **5** (1969) 592.
16. T. R. ZHAO, M. HASEGAWA and H. TAKEI, *J. Crystal Growth*, **154** (1995) 322.

*Received 6 June
and accepted 7 November 1995*